Numerical investigation of coastal circulation around India

S.K. BEHERA and P.S. SALVEKAR

Indian Institute of Tropical Meteorology, Pune-411008, India

(Received 15 July 1996, Modified 3 January 1997)

सार — भारत के समीपवर्ती तटीय क्षेत्र में परिसंचरण का अनुकरण करने के लिए सक्रिय परत वालें वायु वाहित एक सरल महासागरीय परिसंचरण मॉडल का प्रयोग किया गया है। जिन क्षेत्रों की जांच की गई है उनके संख्यात्मक परिणामों के परस्पर अंतः संबंध तटीय परिसंचरण पर वायु का प्रभाव दर्शाते हैं। शीतकालीन ऋतु के महीनों में भारत के पश्चिमी तट के सहारे बहने वाली उत्तराभिमुखी धाराएं बंगाल की खाड़ी के सुदूर प्रणोदन द्वारा प्रभावित हैं। तथापि ग्रीष्मकालीन महीनों के दौरान दक्षिणाभिमुखी धाराएं सुदूर प्रणोदन से कम प्रभावित होती हैं। तट पर रूकी हुई जो कैल्विन तरंगें सुदूर प्रणोदन अनुक्रिया को बढ़ाती हैं वे बंगाल की खाड़ी की स्थानीय पवनों में वार्षिक-चक्र द्वारा उत्पन्न होती हैं। भूमध्यरेखीय तरंगें पश्चिमी तट परिसंचरण को सही प्रावस्था प्रदान नहीं करती हैं। मालदीव तथा लक्ष्यद्वीप की द्वीप श्रृंखलाएं मॉडल परिसंचरण को विशेष रूप से प्रभावित नहीं करती हैं। किन्तु यह मॉडल की ज्यामिति से श्रीलंका को हटाने से ग्रीष्मकालीन महीनों के दौरान बंगाल की खाड़ी के उत्तर पश्चिम में परिसंचरण में विशेष रूप से परिवर्तन आता है। इन परिणामों में से कुछ का पता अति-आधुनिक बहुस्तरीय मॉडल अर्थात मैक क्रिएरी 1993 द्वारा पहले ही लगाया जा चुका है। तथापि इस प्रकार के सरल मॉडल की महत्ता पर प्रकाश डालने हेतु इन परिणामों को पुनः प्रस्तुत किया गया है। अतः आगे और विस्तृत अध्ययन के लिए सरल मॉडल का प्रयोग किया गया है।

ABSTRACT. A simple wind driven ocean circulation model with one active layer is used to simulate the coastal circulation around India. The close agreement of numerical results to that of the observed fields indicate the influence of wind on the coastal circulation. The northward currents along the west coast of India during winter months are dominated by remote forcing from Bay of Bengal; however the southward currents during summer months are less influenced by the remote forcing. The coastaly trapped Kelvin waves which give rise to the remote forcing response are found to be produced by the annual cycle in the local wind of the Bay of Bengal. Equatorial waves do not provide the correct phase of west coast circulation. The island chains of Maldive and Laccadive do not affect the model circulation significantly. But the exclusion of Sri Lanka from the model geometry significantly alters the circulation of southwestern Bay of Bengal during summer months. Some of these findings are already shown by sophisticated multilayer models, *e.g.*, McCreary *et al.* 1993. However, some of these results are again reproduced here in order to highlight the significance of such simple model and hence the simple model is used for further detail study.

Key words — Indian Coastal circulation, Reduced gravity model, Role of small islands.

1. Introduction

The dynamically rich north Indian Ocean has been providing an excellent opportunity for ocean circulation studies. As a result, there have been considerable research work (both observational and theoretical) reported about the various aspects of the hydrodynamical characteristics of the region. The upper north Indian Ocean is mostly influenced by the annually reversing monsoon winds of the region. The strong winds force the ocean locally which in turn excites propagating signals (in terms of Kelvin and Rossby waves) that travel large distances to influence the ocean remotely (Yu *et al.* 1991, McCreary *et al.* 1993 hereafter referred as MKM).

Extensive observational and modelling studies have been attempted relating to the problems of northwestern sector and the equatorial Indian Ocean but relatively less efforts have been made so far to understand the physical and dynamical processes in the Bay of Bengal and coastal region around India. It seems that the coastal circulation plays an important role, in the linking process between Arabian Sea and Bay of Bengal, Ship drift observations (Rao *et al.* 1991), satellite derived inferences (Legeckis 1987) and model results (Potemra *et al.* 1991 and MKM) indicate a southward

boundary current along east coast of India during winter months. The observed surface flow is northward along west coast during the same period (Shetye and Shenoi 1988, hereafter referred as SS). These coastal currents, together with the North Equatorial Current (NEC) south of Sri Lanka, provide a basis for a linking mechanism, Moreover, the northward currents along west coast during northeast (NE) monsoon, discard the direct forcing mechanism by the alongshore winds. But reverse phenomenon occurs during summer months and the currents from west coast (southward) to east coast (northward) complete the coastal circulation.

Remote forcing mechanisms play an important role in determining the circulation features around the Indian coast. The model results of Potemra *et al.* (1991) and Yu *et al.* (1991), have shown that the Rossby wave radiated from the east Bay of Bengal trapped Kelvin wave, determines to a large extent, the current patterns along east coast of India. The coastal Kelvin wave in turn has resulted from eastward travelling equatorial Kelvin wave, generated by the reversing monsoon winds. The modelling study of MKM suggests a more dominating local wind forcing on the east coast of India circulation and that the currents along west coast of India are mostly affected by the remote forcing from Bay of Bengal throughout the year, by the propagation of coastally-trapped Kelvin waves. Although these modelling studies have given a basis for the understanding of the dynamical mechanisms responsible for the coastal circulations and the linking process, there still exist some unsolved questions.

The upper layer circulation features around the Indian coasts are well simulated using a simple wind-driven reduced gravity one active layer ocean circulation model. The simple model could reproduce most of the observed general circulation features and other findings obtained from more sophisticated multi-layer models. The advantage of using such simple model with less dynamics and physics is the easy and definite way of interpreting the results and easier way of addressing certain forcing mechanisms. An attempt is made to investigate the influence of remote forcing on the currents along both the coasts of India and some sensitivity experiments are carried out with idealised wind stress forcing to understand, which part of the wind field can generate such remote forcing response. Small islands generally are not resolved by the coarse resolution Ocean General Circulation Models. The role of such exclusion if any on the model circulation features is also investigated by including the island chains of Laccadive and Maldive in the present model geometry.

2. The model

The model used in this study has one active layer, overlying a deep motionless inactive layer, *i.e.*, zero pressure gradient in the lower layer which effectively filters the fast barotropic mode. The model equations are based on vertically integrated shallow water equations over a layer, assuming no vertical shear in horizontal fields.

Luther *et al.* (1985), Simmons *et al.* (1988), Luther and O'Brien (1989) have shown that such a reduced gravity model can realistically simulate most of the circulation features in the Indian Ocean.

The model equations in Cartesian co-ordinate are :

$$U_t + (UU/H)_x + (UV/H)_y - fV + (g'/2)(H^2)_x = A_H\nabla^2(U) + \tau_{xz}/\rho_1 \quad (1)$$

$$V_t + (UV/H)_x + (VV/H)_y + fU + (g'/2)(H^2)_y = A_H\nabla^2(V) + \tau_{yz}/\rho_1 \quad (2)$$

$$H_t + U_x + V_y = W_e \quad (3)$$

where U and V are zonal and meridional components of transport obtained from vertically integrating upper layer velocity field, f is the Coriolis parameter ($2\Omega\sin\Phi$). H is the upper layer thickness, $g' = g(\rho_2 - \rho_1)\rho_2$ is the reduced gravity. A_H is the horizontal eddy viscosity coefficient and τ_{xz}, τ_{yz} are the components of the wind stress applied as a body force. W_e is a source term representing entrainment from deep motionless layer to the upper active layer. This entrainment is introduced only to prevent the interface from surfacing that happens when a small initial upper layer thickness is considered. This term is positive for upper layer in case layer thickness becomes less than a pre-set minimum depth H_{min}. The term is determined through a simple function as suggested in McCreary and Kundu (1988).

The effect of this entrainment on the upper layer density, momentum and kinetic energy balance has been neglected. It is assumed that the entrained water engulfed into the upper layer, has zero velocity and is instantaneously adjusted to the density ρ_1. The values of various parameters and constants used in this study are listed in Table 1.

The model equations are solved numerically on a finite difference mesh staggered in space (Arakawa C-grid) and integrated with respect to time using leap-frog finite-difference scheme. An Euler scheme is applied at every 49th step to eliminate the spurious growth that usually arises due to time-splitting in leap-frog scheme. The horizontal domain used in the model extends from 35°E to 115°E and from 24°S to 23°N (Fig.1). Boundary conditions are noslip ($U = V = 0$) at land boundaries and modified radiation boundary condition (Camerlengo and O'Brien 1980, Jensen 1990) is applied at the open boundaries. However, the model results over 65°E to 90°E and Equator to 23°N alone are presented here in order to discuss the circulation around Indian costs.

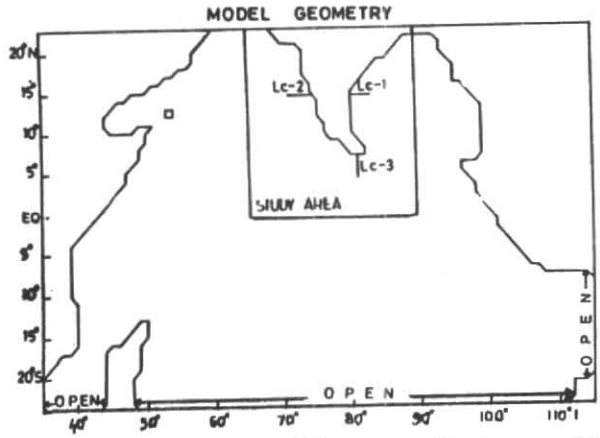

Fig.1. The north Indian ocean model geometry and the study area of the present work

TABLE 1
Parameters used in the model

Parameters	Symbol	Value
Reduced gravity	g'	0.03 ms^{-2}
Initial upper layer thickness	H_o	200 m
Initial phase speed	$C_o=(g'H_o)^{1/2}$	2.45 ms^{-1}
Minimum upper layer thickness	H_{min}	75 m
Entrainment time	τ_c	8 hr
Eddy viscosity coefficient	A_H	2250 m^2s^{-1}
Grid length	ΔX and ΔY	28 km
Time step	Δt	30 min
Density(air)	ρ_a	1.2 kg m^{-3}
Density(water)	ρ_w	1026 kg m^{-3}
Drag coefficient	C_D	$1.25*10^{-3}$

3. Input data

Monthly mean pseudo wind stress values at 1 degree interval are obtained from FSU (Legler *et al.* 1989) for the period 1977 to 1986. The pseudo stress components are converted into stress components being input to the model using a constant drag coefficient C_D and air density ρ_a. A bi-cubic spline technique is then used to interpolate the input values at model grid points.

We assume that the monthly mean wind data represents the value at the middle of the respective month and then linearly interpolated between adjacent months to get the data at model time step. For simplicity, model calendar is considered to be of 360 days and each month of 30 days.

4. Results and discussion

Some of the results presented here are also reported by sophisticated multi-layer models. However, it is found that simple model could reproduce most of the features and hence for detailed investigation the simple model is used.

4.1. *Annual cycle of the model currents*

In this sub-section the simulated annual cycle of the circulation features after ten year of model integration around the Indian peninsula are discussed and compared with the available observed features (Rao *et al.* 1991). In general, the model-simulated currents are under-estimated as compared to the ship drift observations, as the model currents are depth-averaged values of the upper layer (that has an initial depth of 200 m). The model results shown in the figures are instantaneous snapshots of the middle of the respective months.

In January, the surface winds over the region are north-easterlies and the stress curls are negative (positive) near east (west) coast [Figs.2(a & b)]. The circulation, as seen from Fig.2(c), indicates northward flow off the west coast of India (north of 11°N). Infact, the numerical solution indicates northward flow throughout November to February. The strong northward flow is seen away from the coast in January, because of the faster westward spreading of northward flow for the assumption of higher initial upper layer thickness H_o. This discripancy vanishes when the H_o is reduced upto 100 m (for details please see section 4.1.1). The flow field towards south is much wider because of offshore propagation of Rossby waves (MKM), evident from the upper layer thickness fields (shown in terms of deviation from H_o, hereafter ULT) shown in Fig.2(d). An anticyclonic eddy is also seen around 8°N and 73°E as reported by Bruce *et al.* 1994, which has changed northward coastal circulation to southward, south of 11°N. The northward flow, to some extent can be attributed to the local wind stress curl over the Arabian Sea (Sverdrup dynamics), but the remote forcing mechanism in terms of coastal Kelvin wave radiated from Bay of Bengal seems to be dominating mechanism, as suggested by MKM. The simple one active layer model in our case could also produce the same result.

The circulation along east coast of India is dominated by a northward flow north of 13°N and the flow is southward south of it. Onshore flows around this latitude feed into these flows. Computer animation of Bay of Bengal circulation suggests that the northward flow has propagated from the eastern rim. There exists a cyclonic eddy off the coast of Madras, which is in agreement with many numerical results, *e.g.*, MKM and is not exclusively investigated so far. The flow south of Indian peninsula and Sri Lanka is dominated by NEC, which agrees well with observations.

In May, winds over most part of the basin have become southwesterly and positive curl dominates the southern part of the coastal region [Figs.3(a & b)]. Along the west coast of India the local alongshore wind is equatorward and along the east coast it is northward. The ship drift observations suggest a southward flow along the west coast that appears in March and continues upto September with a peak strength in July. The model currents [Fig.3(c)] support these obser-

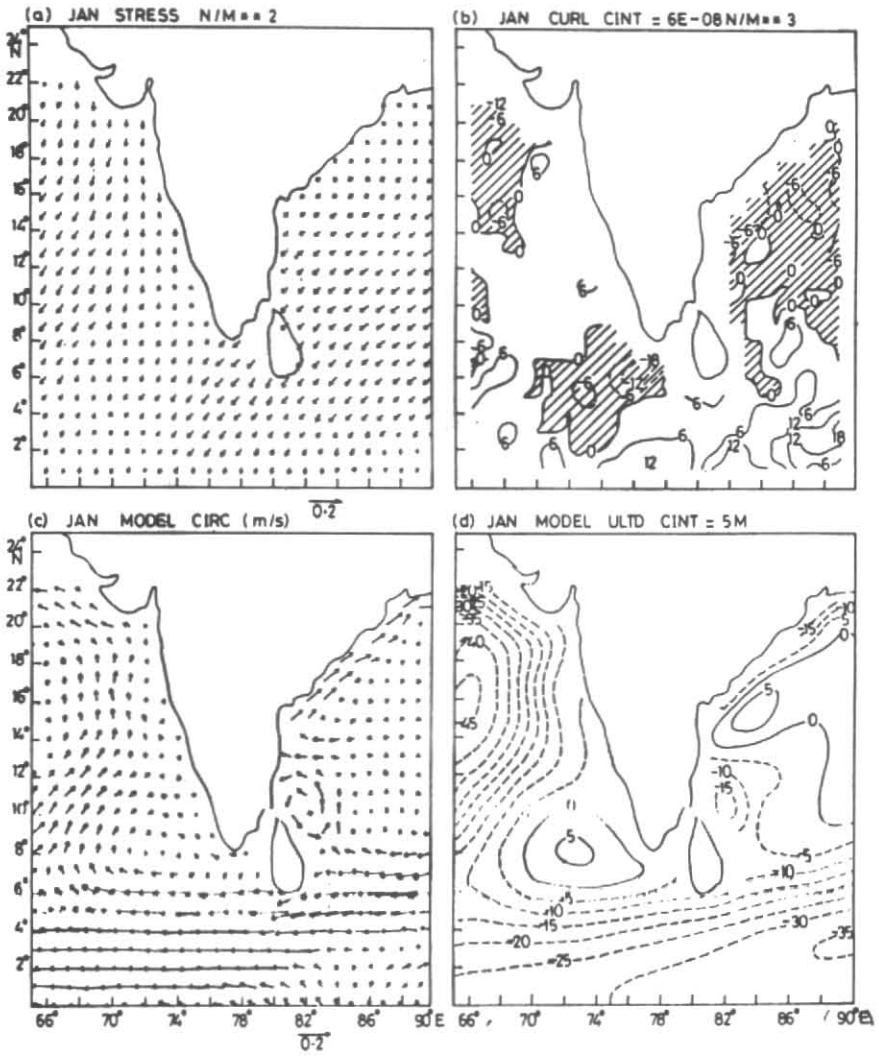

Figs.2(a-d). Mean January (a) wind stress, (b) its curl (contour interval is $6*10^{-8}$ N/m^3), (c) Model circulation and (d) upper layer thickness (contour interval is 5m)

vations. SS have suggested an equatorward flow along the west coast in response to the local alongshore wind. The northward flow along east coast is now restricted upto 18°N and the offshore flow turns back to form an anticyclonic gyre off the coast of Andhra Pradesh. The flow is equatorward along the east coast of Sri Lanka which is a part of cyclonic gyre in the south eastern Bay. The NEC in May is replaced by eastward monsoon current to the south of Sri Lanka.

In July, the southwest monsoon winds reach peak strength and the stress curl has become negative (positive) near the west (east) coast as seen in the Figs.4 (a &b). As a result of strong alongshore wind there is strong upwelling as indicated by the further shallowing of the ULT all around coast of India [Fig.(4d)]. This shallow ULT also spreads off the west coast of India indicating the westward propagation of Rossby waves. The flow along the west coast continues to the south and is stronger and wider than that in May. The southward flow along the east coast of India [Fig.4(c)] differs with ship drift observations, because the ship drift observations are restricted to the currents in the upper few meters of the ocean (mostly Ekman flow) whereas the model-produced currents are the depth-averaged flow of the upper 200 meter. However, SS have suggested a southward coastal current along east coast as a Munk layer solution in response to the northward interior Sverdrup flow forced by the positive wind stress curl in the interior basin. Animation of the model results from Bay of Bengal, suggest that the model-produced southward flow has been propagated from the eastern rim of the Bay. It is already reported that four major forcing mechanisms influence the dynamics of East India Coastal Circulation (EICC), namely : (a) local alongshore wind, (b) remote alongshore winds, (c) remote for-

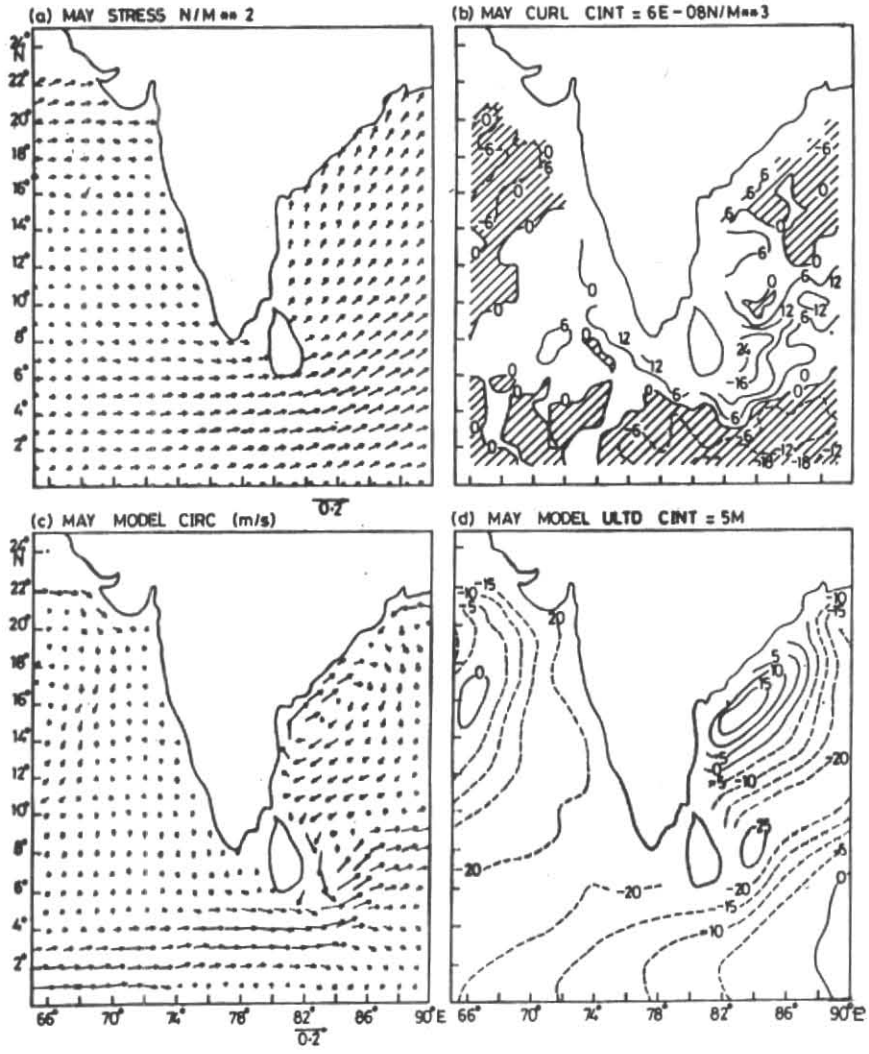

Figs.3(a-d). Same as Fig.2 except for May

cings from equator and (d) Ekman pumping in interior Bay. McCreary *et al.* (1996) investigated these four mechanisms by numerical solution. They have suggested that along the Indian coast (north of 10°N), the surface EICC flows north eastward from February until September, with a peak in March-April and weaker flow in June to September. The interior Ekman pumping, remote alongshore winds and equatorial forcings found to contribute to the spring-time peak and local alongshore winds found to be the driving force of the weaker summer-time flow in their case. In addition to these, we found the opposite influence of equatorial remote forcings (details given in sec.4.2.2). The cyclonic gyre of May [Fig.3(c)] has moved towards northwest and there are two cyclonic eddies embedded in it, among which the eddy off the coast of Madras is the counterpart of the eddy that was present during NE monsoon. Both the eddies persist upto August and decay in September. The eastward monsoon currents persist south of Sri Lanka.

The southwest monsoon collapses by October and in November northeasterlies set in over most part of the region with positive wind stress curl along both the costs [Figs.5(a&b)]. The equatorward flow along the west coast, which was present upto September, changes its direction towards north in October and is northward all along the coast in November [Fig.5(c)]. The ULT field [Fig.5(d)] shows deepening along both west and east coasts as compared to the monsoon months. This model feature supports the dominating influence of remote forcing on the west coast circulation through the spreading of downwelling coastal Kelvin waves from Bay of Bengal, as suggested in MKM. The equatorward flow along the east coast is confined to a very

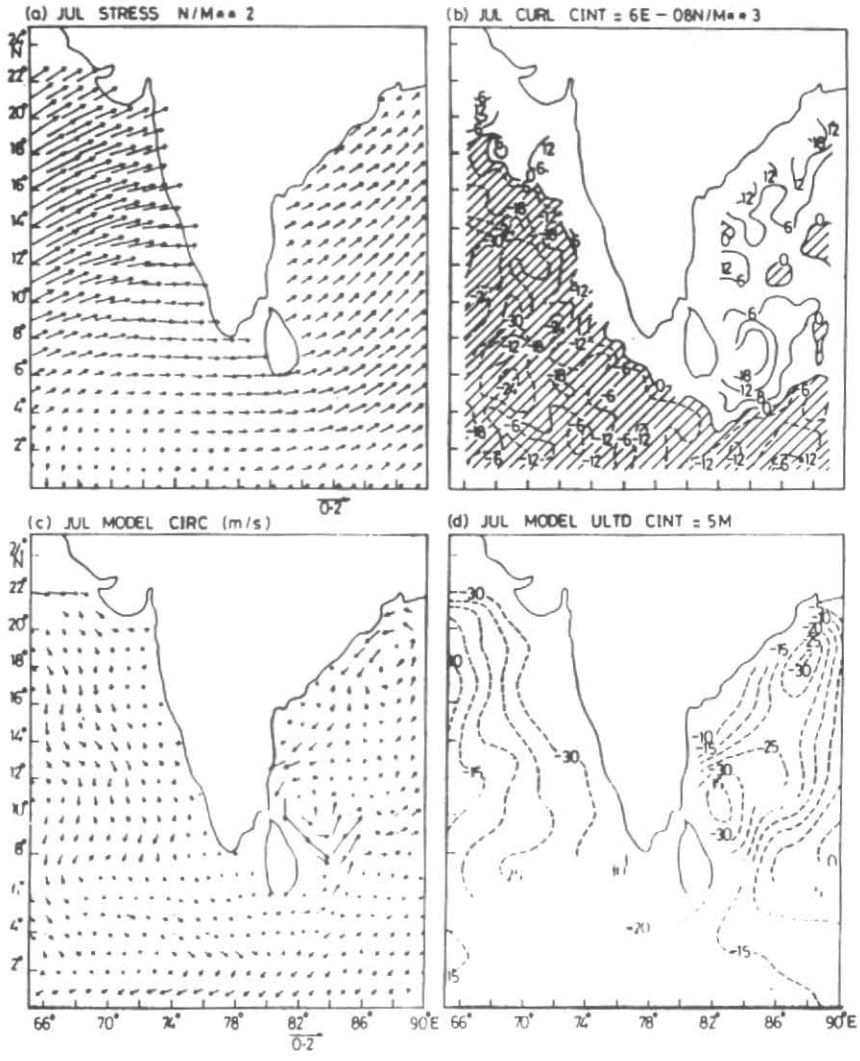

Figs.4(a-d). Same as Fig.2 except for July

narrow band, little away from the coast, currents are northward.

Near to south of Sri Lanka, the monsoon currents are replaced by the westward flow, whereas away from the coast the eastward flow persists. The southward flow along the east coast, the westward flow south of Sri Lanka and the northward flow along the west coast together with the ULT field, strengthen the idea of remote forcing mechanism on the west coast circulation.

4.1.1. *Near surface currents*

Model currents reported earlier differ with observed ship drift currents, mostly along east coast. We examined the model deficiency in producing the observed surface currents by reducing the model initial upper layer thickness to 100 m from the previous value of 200 m. This change in model parameter will give rise to a slower mode with initial phase speed of C_0 = 1.73 m/s. The model simulated annual cycle of currents are shown in Fig.6. Currents along both the coasts have considerably improved to that discussed in previous section. Northward (southward) currents found all along the west (east) coast in January [Fig.6(a)] which are in agreement with ship drift currents. The change in the two results is due to the slower propagation of downwelling Rossby wave in the latter case. This has resulted in a slower westward propagation of northward currents along west coast. The northward currents are found near coast in November and have not spread much to west in January [Figs.6(a & f)], compare with Figs.2(c) & 5(c)]. The southward currents could continue all along east coast because of the slower propagation of northward flow from eastern rim of Bay [Figs.6 (a & b)]. There are weak northward currents found along the east coast in March and in May they become stronger which is consistent with observational evidences.

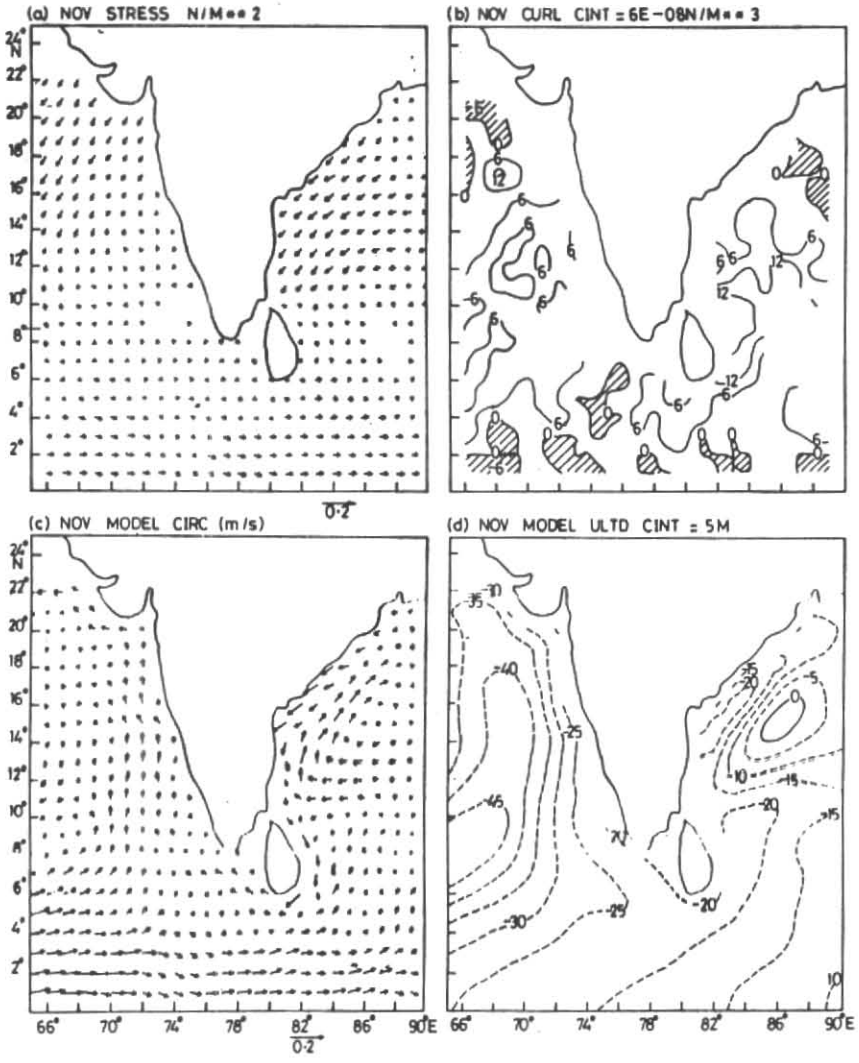

Figs.5(a-d). Same as Fig.2 except for November

The local forcing by the alongshore wind may not be playing a dominant role for the onset of the northward flow along the east coast in May which is evident from the westward propagation of the northward flow [Figs. 6(a-c)].

However, this model experiment also could not produce the observed northward coastal currents along east coast in July [Fig.6(d)]. The model deficiency can be attributed to the shallow near surface structure of the coastal circulation along the coast. The Rossby wave propagation in the equatorial wave guide is also evident. from [Figs. 6(d & e)], which produces high variability in the eastward monsoon current south of Sri Lanka as suggested by Schott *et al.* 1994. Southward currents reappear along the east coast in September and are stronger in November [Fig.6(f)] that are consistent with observational evidences.

4.1.2. *Transport along the coast*

The mass transports, computed at three locations around the coastal region (Lc-1, Lc-2 and Lc-3 as seen in Fig.1) for both, 200 m & 100 m initial depth cases, are discussed in this subsection. Time series of transports and the wind stress components are shown in Fig.7. At locations Lc-1 and Lc-2, meridional stress components may be considered as pseudo alongshore stress that can directly force alongshore currents and zonal stress components may be considered to give rise to alongshore Ekman transport, where as at location Lc-3, *vice versa* is true. Time series of transports at all the three locations shows dominance of an annual cycle.

At location Lc-1, in the case of 200 m initial depth, (hereafter first case) the meridional transport is northward from December to May with a maximum (max.) of 10 Sv in

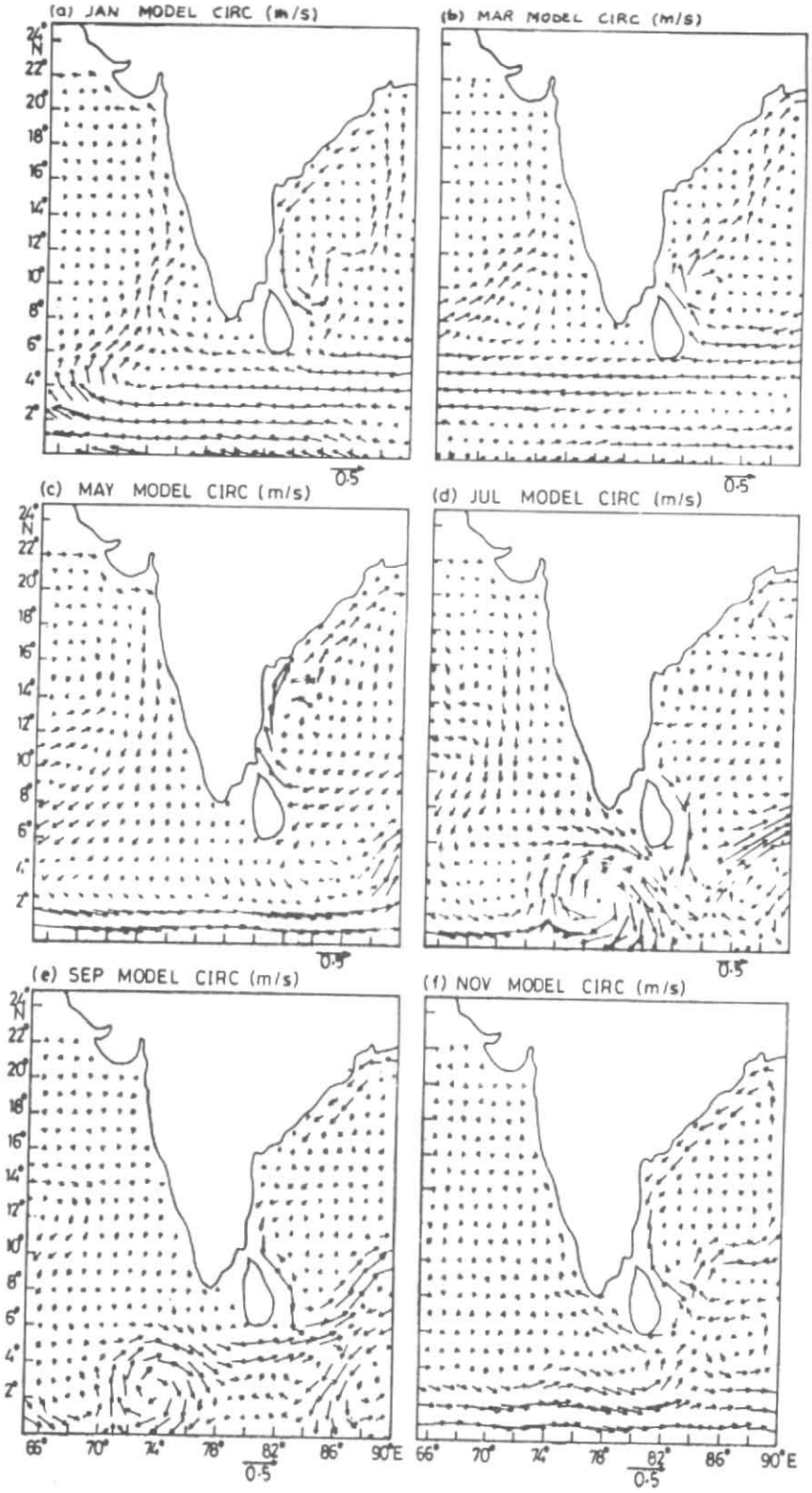

Figs.6(a-f). Model circulation fields in case of the 100m initial depth. (a) January, (b) March, (c) May, (d) July, (e) September and (f) November

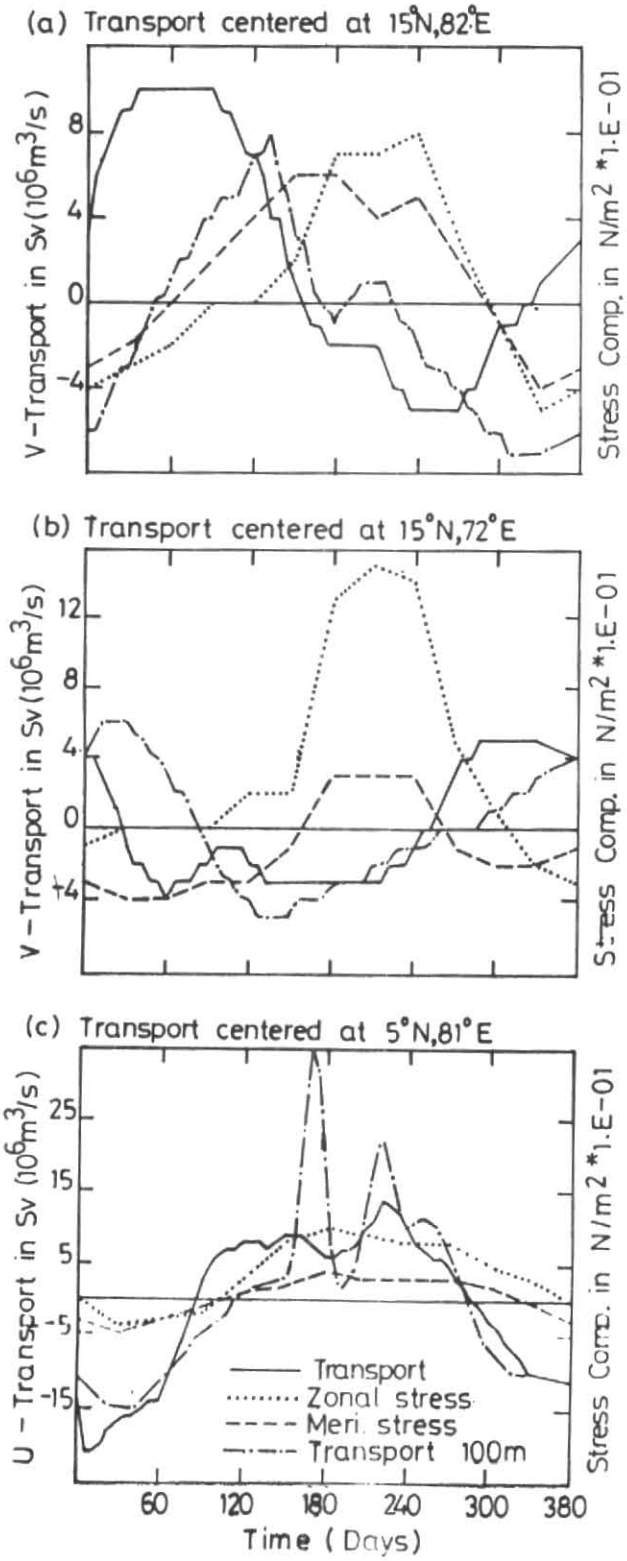

Figs.7(a-c). Time series of Mass transport for both 200 m and 100m initial depth cases together with the zonal and meridional components of wind stress at (a) Lc-1 centered at 15°N & 82°E, (b) Lc-2 centered at 15°N & 72°E and (c) Lc-3 centered at 5°N & 81°E.

March and is southward from June to October with a maximum of 5 Sv in September. Since the transports are in opposite phase with zonal stress components the influence of Ekman transport is indicated. The transport, in the case of 100 m initial depth, (hereafter second case) shows phase shift from first case in both northward & southward, obviously due to the slower baroclinic mode. The meridional transport is northward from March to August with a primary maximum of 8 Sv in May. Transport is southward from September to February with a maximum of 7 Sv in November-December.

At location Lc-2, in the first case, the transport is northward from September to January (max. 5 Sv in Nov-Dec) and southward from February to August (max. 4 Sv in March). In the second case, the transport is northward from October to April (max. 6 Sv in February) and is southward from May to September (max. 5 Sv in June). The precedence of the phase of the northward and southward transports to the zonal stress in both the cases suggest a less important role of local Ekman dynamics. The maximum southward transport at Lc-1 precedes the phase of northward transport at Lc-2 in both the cases.

At location Lc-3, in the first case, transport is westward from November to April (max. 21 Sv in January) and is eastward from May to October (max. 15 Sv in September). In the second case the direction of zonal transports remain almost same to that of first case, except for enhancement in the magnitude. The phase differences in zonal transports, between the two cases are negligible at Lc-3. The high fluctuations found in the amplitude at Lc-3 may be due to the westward propagating reflected equatorial Rossby waves.

Meridional components of wind stress are out of phase with transports at Lc-1 & Lc-2 in both the cases, which indicate the negligible role of local alongshore wind on the model flow field. Although, they are in phase at Lc-3, these components may be playing a less important role at that location. The general agreement between the model zonal transports and the zonal stress components at Lc-3 suggests the influence of local forcing in that region. Schott *et al.* (1994) have calculated currents and transports from moored current measurements and ship board profilings, south of Sri Lanka. The locations for the moored array, is close to our model location Lc-3. The calculated time series of zonal transport in the upper 300 m, yields transport fluctuations in the range of 25 Sv westward to 24 Sv eastward (Fig. 7 from Schott *et al.* 1994). Further, the direction of transport is same as reported in the present study (*i.e.*, westward during November to April and eastward during other months).

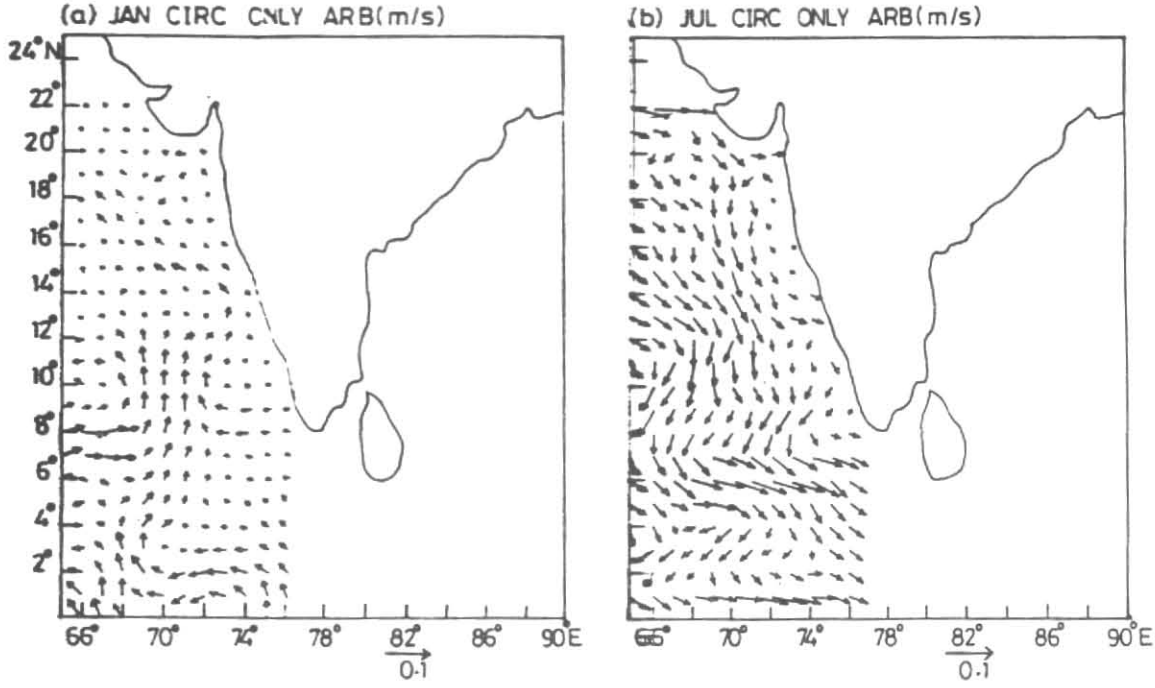

Figs.8(a-b). Model circulation for (a) January and (b) July, when model geometry is only upto 77°E

4.2. *Forcing mechanisms*

The model results discussed in previous sections suggest the influence of different local and remote forcings on the model circulation features. In this section, results of some idealised numerical experiments are discussed to further strengthen the earlier suggested forcing mechanisms.

4.2.1. *Arabian Sea wind*

In this experiment, the model geometry is modified to exclude the eastern half of the basin, *i.e.*, the model domain become 35°E-77°E and 24°S-23°N and the open boundary condition is applied at 77°E. It is similar to Arabian Sea wind case of MKM, except that the exclusion of the eastern half of the basin in our case will completely isolate the west coast model solutions from the influence of coastal Kelvin waves, propagating from Bay of Bengal, hence will provide a concrete conclusion. The circulation in January [Fig.8(a)] shows a very weak northward flow along the west coast as compared to that in the main run [Fig.2(c)]. However, currents in July [Fig.8(b)] are replication of the main run [Fig.4(c)]. This brings out the clear dominating influence of remote forcing from Bay of Bengal on the West coast circulation in winter months and not so significant influence in summer months.

4.2.2. *Idealised wind forcings*

In order to understand further, which region of wind forcing can lead to the remote forcing response on the west coast circulation; a series of sensitivity experiments are carried out with idealised wind forcings. The wind forcings are considered for West Equatorial Region (WER, 55°E & 5°S to 5°N). East Equatorial Region (EER, 85°E & 5°S to 5°N), Bay of Bengal Region (BBR, 7°N) and Bay of Bengal & East Equatorial Region (BBER). Unlike the real wind experiments in MKM, in this case the time series of wind stress fields are generated using a simple Sine function similar to Yu *et al.* (1991). for easy interpretation of model responses.

$$\tau_{xz} = -\tau_o \sin(\sigma t) \qquad (4)$$

$$\tau_{yz} = -\tau_o \sin(\sigma t) \qquad (5)$$

where the amplitude $\tau_o = 0.1\ Nm^{-2}$ that reduces to zero at the edges with Sine tapper, having band width 9°. The frequency $\sigma = (2\pi/360$ days) can be considered to be the annual reversal of monsoon winds in a simpler way. In the west equatorial and east equatorial cases, the meridional stress component is neglected. A spin-up time of 3 years is allowed in each of these cases and the results from 4th year are discussed. In order to enhance the weak flows compared to strong flows, the current arrows are plotted from the

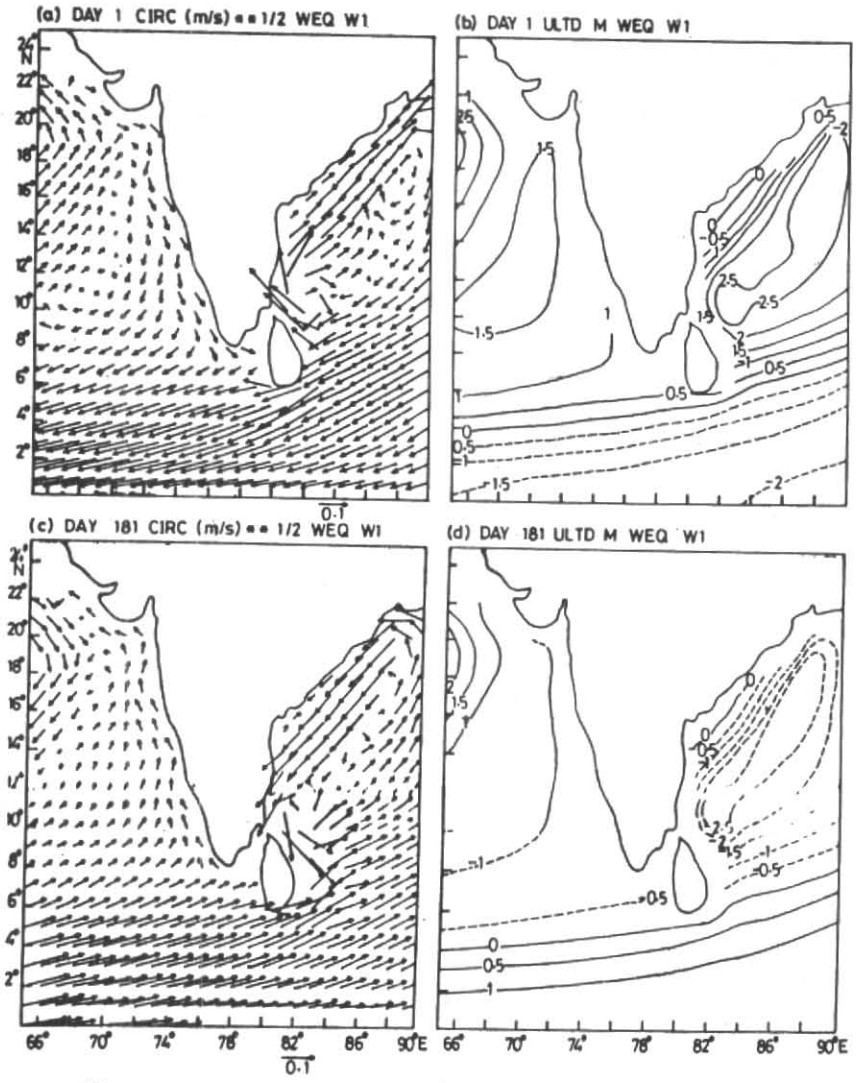

Figs.9(a-d). Circulation [$V = V/(V)^{1/2}$] and upper layer thickness for west equatorial wind case. Contour interval is 0.5m., (a) & (b) for January and (c) & (d) for July

vector field $V = V/(V)^{1/2}$, that has same direction as V, but has amplitude of $(V)^{1/2}$.

Fig.9(a) shows the currents at day 1 from the 4th year of model integration in WER case. The currents are northward along east coast and southward along west coast. The ULT fields [Fig.9(b)] show the shallowing of upper layer along the west coast (in response to the coastal Kelvin waves, radiated from Bay of Bengal). The southward currents further strengthen and spread westward in the following 90 days and then weaken. At day 181, northward currents begin along the west coast with the westward radiation of low ULT field off the coast and the deepening of ULT along the coast [Figs. 9(c &d)]. Currents are southward along the east coast. It is found that the northward west coast currents become stronger and spread westward in next two months, hence later the coastal flow became weak after day 300, to be replaced by the southward currents at the end of the year.

The above experiment could show the influence of equatorial waves, generated by a patch of equatorial wind field on the coastal circulation far away from the forcing region. The phases of northward and southward currents along both the coasts are exactly opposite to what is expected in that part of the year, which can be explained in the following manner.

As the westerlies weaken after day 300 (peak at 270th day), an upwelling Kelvin wave is generated which then propagates to the eastern coast in a few weeks. The upwelling signal radiates along the peripheri of Bay of Bengal and then passes on to west coast as coastal Kelvin wave. As a result southward currents set in along the coast towards end of the year. Opposite phenomenon occurs at the end of

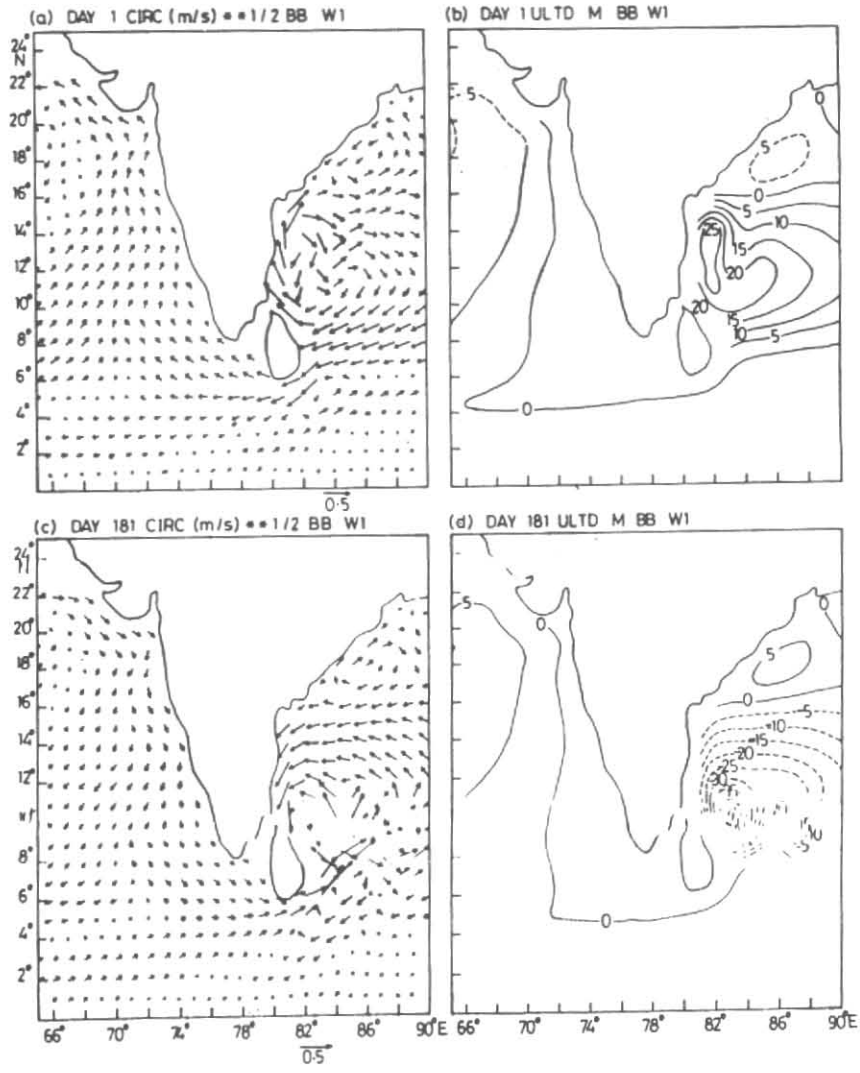

Figs.10(a-d). Same as Fig.9, but for Bay of Bengal wind case. Contour interval is 5m

easterly wind phase. The circulation along east coast is influenced by yet another mechanism, *i.e.*, the westward propagation of downwelling and the upwelling Rossby waves from the eastern rim of the Bay. The synchronisation of a downwelling coastal Kelvin wave and an approaching upwelling Rossby wave, originated six month earlier and propagated to the east coast at day 181 (and the reverse condition at day 1) has provided a stronger zonal pressure gradient that has resulted into stronger currents along east coast.

The east equatorial wind forcing produces essentially similar model results as discussed for west equatorial wind case, except for a few weeks precedence.

Fig. 10 shows the currents and ULT fields at day 1 and at day 181, in the BBR case. The currents along west coast are northward at day 1 [Fig.10(a)] and the southward at day 181 [Fig.10(c)]; exactly opposite from the results of WER case. The northward currents start from day 301 and continue upto day 61 of the next year. The southward currents start from day 121 and continue upto day 241. The onset of these currents coincides with the radiation of coastal Kelvin waves from Bay of Bengal. These currents strengthen and spread westward with the spreading of ULT fields [Figs. 10(b & d)] in subsequent months. Computer animation of model fields yields the following inferences.

In response to the northeasterly winds and the negative wind stress curl generated by the truncation in the wind field, the upper layer of the northern Bay deepens whereas the upper layer becomes shallow in the southern Bay. As the strength in the northwesterlies weaken after day 90, (not

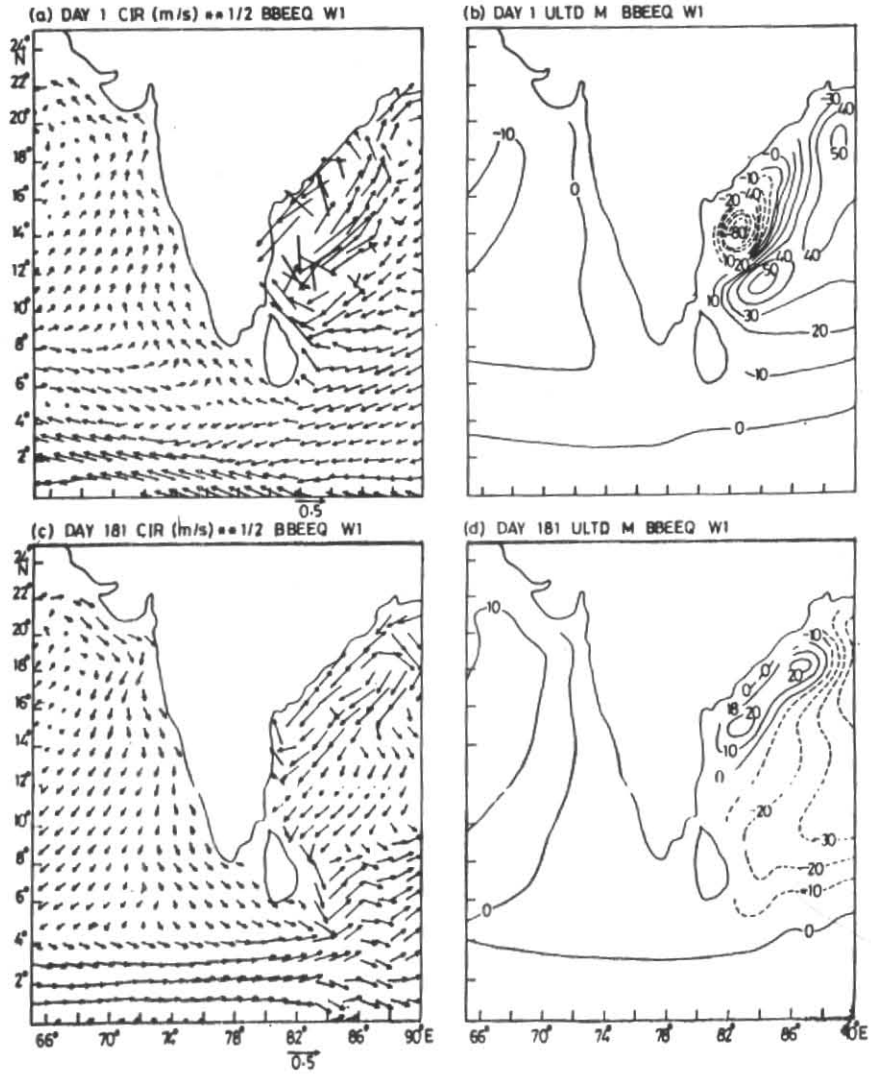

Figs.11(a-d). Same as Fig.9, but for Bay of Bengal and east equatorial wind case. Contour interval is 10 m

shown) upwelling coastal Kelvin wave starts propagating from the southwestern Bay, that sets in the southward coastal currents along west coast. A reverse phenomenon occurs after day 270 (peak of southwesterlies). The general agreement between the phase of the currents in this experiment with that of the model results in the main run indicates the importance of remote forcing response on west coast circulation induced by the Bay of Bengal wind.

The truncation in the wind field affected the east coast circulations and hence this is not discussed. However, the truncation did not have any impact on the west coast circulation which is demonstrated in the next experiment.

Previous sensitivity experiments suggest that the remote forcing produced by the Bay of Bengal wind is the most appropriate reasoning to explain the west coast circulation. Further, in order to understand the dominance of these wind forcing responses, over one another, some more experiments are carried out. Fig. 11 shows the model solutions at day 1 and at day 181 in BBER case.The circulation and ULT fields along west coast are in general, good agreement with the previous case. However, shift in the truncation of the wind field has changed the model solutions along east coast. The model solutions along west coast from this experiment are in opposite phase to that of the only equatorial wind forcing cases. This indicates the dominance of Bay wind forcing response over the equatorial wind forcing response, in shaping the west coast currents. From the animation of events that take place from day 1 to day 360, the following inferences are drawn.

In response to the southwesterly wind (after day 270), the upper layer of the northwestern sector of the Bay shallows and that in the southeastern sector deepens. The higher ULT fields radiate westward by Rossby wave propagation

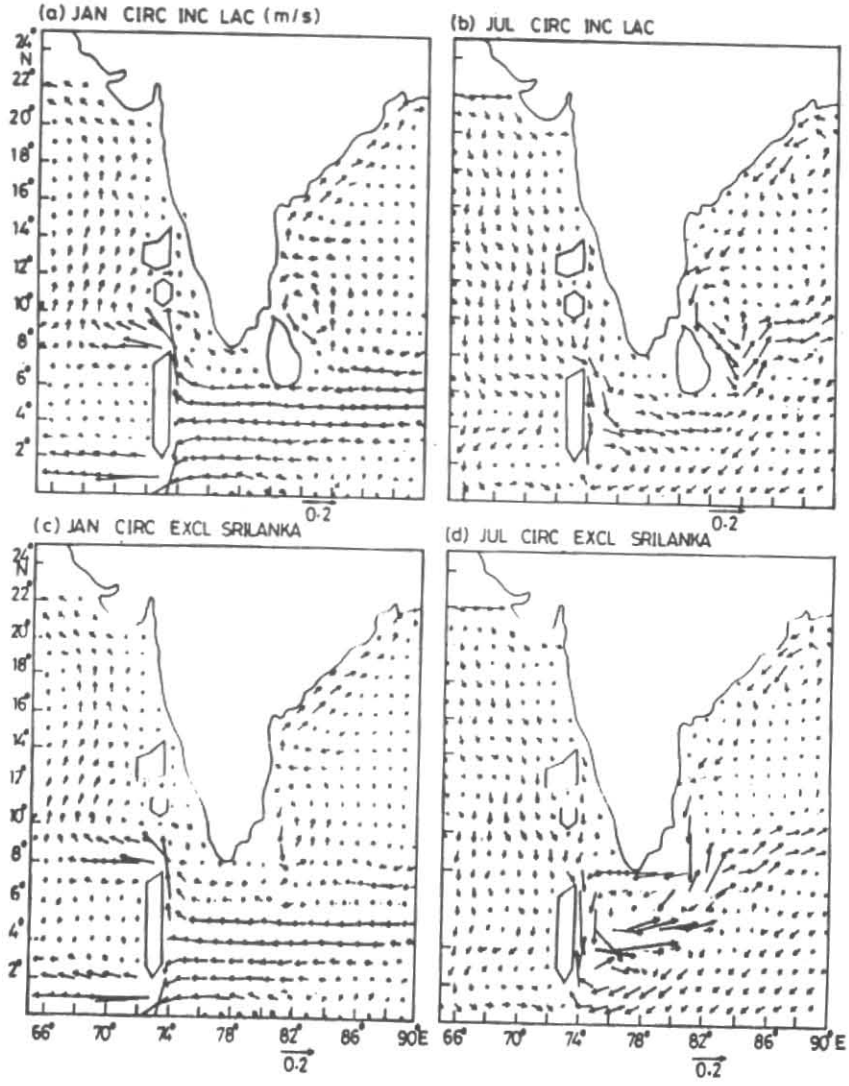

Figs.12(a-d). (a) Model circulation for January, when Laccadive and Maldive Island chains are included in the model geometry, (b) Same as (a) but for July, (c) Model circulation for January when Sri Lanka was excluded from model geometry and (d) Same as (c) but for July

from eastern rim of the Bay. The higher ULT fields are seen off the coast of Madras at day 1 [Fig.11(b)]. The changes in this higher ULT, help in radiation of coastal Kelvin wave to the west coast. The higher ULT fields also block the radiation of lower ULT fields from the northeastern sector. This blocking mechanism was not available in the case of only equatorial wind forcing cases. A similar, but opposite in amplitude phenomenon occurs during the rest of the year.

Similar model solutions are obtained when east equatorial wind was replaced by west equatorial wind. Also, experiments with less intense Bay wind produce similar results.

4.2.3. *Influence of islands*

Most of the small (Islands around India are not resolved in coarse resolution ocean models. In this sub-section we will discuss the influence of such islands like Laccadive and Maldive Island chains on the large scale circulation of the region. The monthly mean FSU wind stresses are used as forcing in these experiments.

In the first experiment the Laccadive and Maldive Islands are included in the model geometry in order to determine their effects on the equatorial current structure, south of Indian peninsula and specially on the Laccadive High (Bruce *et al.* 1994), which is present during winter months. The NEC has been splitted up by the Maldive Islands during January [Fig.12(a)] with a stronger flow in the channel between Maldive and Laccadive Islands [as compared with Fig.2(c)]. During July the structure of the Laccadive High and coastal circulation [Fig.12(b)] along the coast of Kerala are slightly affected by the presence of the Islands.

In another experiment the Sri Lankan Island was removed from the model geometry to understand its effect on the circulation off the coast of Madras, specially on the two cyclonic eddies that arise during January and July. In the January circulation [Fig.12(c)], the cyclonic eddy is still present off the coast of Madras, which indicates minor role being played by the Island for the formation of the eddy. However, the July circulation [Fig.12(d)] clearly indicates the dominant role of Sri Lanka in the formation of the cyclonic eddy. In the absence of the blocking mechanism, the cyclonic circulation has moved down to the south of the tip of Indian peninsula. The westward propagation of the eddy was blocked by the Maldive Islands.

5. Conclusions

The simple wind driven ocean circulation model with only one active layer is able to simulate most of the observed circulation features around the Indian coastal region throughout the year. The variation between observed currents and the model simulated currents along the east coast of India during mid summer months is mainly due to the shallow near-surface ship drift currents as compared to the model depth-averaged flows. Model results from a shallow initial depth experiment show improvement in the east coast circulation. Computed mass transport at a location along east coast is northward during December to May and is southward in other months in case of 200 m initial depth. The transport is northward from March to August (with a brief southward phase in July) and is southward in other months, in case of 100 m initial depth. The maximum southward mass transport along east coast precedes the start of northward transport along west coast that indicates a linking process between the two basins. The model produced transports of the section south of Sri Lanka is in qualitative agreement with observed transports.

The remote forcing response on the currents along west coast of India from the Bay of Bengal through propagation of coastal Kelvin waves has been demonstrated in idealised experiments. Experiment, in which the model geometry was considered only upto 77°E, the northward currents along west coast of India, in winter months; were considerably reduced in amplitude. However, the currents in summer months were not affected; which suggest a dominating role of remote forcing on west coast circulation in winter months and a less dominance in summer months. Further, idealised wind forcing experiments, suggest a dominating influence of Bay of Bengal wind over the equatorial wind in producing the remote forcing response on west coast circulation. In particular, the equatorial waves are found to produce opposite phases of east and west coast current. The Bay of Bengal wind provides a blocking mechanism through Ekman dynamics resulting the westward propagation of Rossby waves which does not allow the out of phase propagation of ULT produced by equatorial forcings to reach west coast.

The Island chains of Maldive and Laccadive do not affect the circulation feature significantly. However, in the absence of Sri Lanka, the cyclonic eddy off the coast of Madras in July is shifted to South. Role of initial upper layer depth on the surface circulation, and the sensitivity experiments to determine the role of different regional forcing mechanisms on the coastal circulation around India are reported for the first time with the simple model. Further the model is being modified to include more active layers and the effect of temperature and salinity which will further improve the circulation features.

Acknowledgements

The authors are thankful to Prof. R.N. Keshavamurty, Director, Indian Institute of Tropical Meteorology, Pune for his interest in the work. They are grateful to Prof. J.J. O'Brien, Dr. J.N. Stricherz, Dr. M.E. Luther for supplying the data and helpful suggestions. They are also grateful to Dr. J.P. McCreary and Dr. S.K. Mishra for suitable comments to improve the manuscript. They are thankful to Miss S.R. Kamble, Mrs. S.S. Naik and Shri D.W. Ganer for typing and preparation of the manuscript.

References

Bruce, G.J., Donald, R.J. and Kindle, C.J., 1994, "Evidence for eddy formation in the eastern Arabian Sea during the northeast monsoon", *J. Geophys. Res.*, **94**, C4, 7651-7664.

Camerlengo, A.L. and O'Brien, J.J., 1980, "Open boundary conditions in rotating fluid", *J. Comp. Phys.*, **35**, 12-35.

Jensen, T.G., 1990, "A numerical study of the seasonal variability of the Somali Current", *Ph.D. dissertation*, Florida State University , 118 p.

Legeckis, R., 1987, "Satellite observations of a western boundary current in the Bay of Bengal", *J. Geophys. Res.*, **92**, C12,12974-78.

Legler, D.M., Navon, J.M. and O'Brien, J.J., 1989, "Objective analysis of pseudostress over the Indian Ocean using a direct minimisation approach", *Mon. Wea. Rev.*, **117**, 709-720.

Luther, M.E., O'Brien, J.J. and Meng, A.H., 1985, "Morphology of the Somali Current system during the southwest monsoon: Coupled ocean-atmosphere models", Ed. J.C.J., Nihoul, Elsevier Science Publ.

Luther, M.E. and O'Brien, J.J., 1989, "Modelling the variability in Somali Current, Meso Scale/synoptic coherent structure in Geophysical turbulence", Eds.J.C.J. Nihoul and B.M. Jamart, Elsevier Science Publ.

McCreary, J.P., Kundu, P.K., 1988, "A numerical investigation of the Somali Current during the southwest monsoon", *J.Mar.Res.*, **46**, 25-58.

McCreary, J.P., Kundu, P.K. and Molinari, R.L., 1993, "A numerical investigation of dynamics, thermodynamics and mixed layer processes in the Indian Ocean", *Prog.Oce.*, **31**, 181-244.

McCreary, J.P., Han, W., Shankar, D. and Shetye, S.R., 1996, "Dynamics of east India coastal current 2. Numerical solutions", *J. Geo.Res.*, **101**, C6, 13,993-14,010.

Potemra, J.J., Luther, M.E. and O'Brien, J.J., 1991, "The seasonal circulation of the upper ocean in the Bay of Bengal", *J. Geophys. Res.*, **96**, 12,667-12,683.

Rao, R.R., Molilnari, R.L. and Festa, J.F., 1991, "Surface meteorological and near surface oceanographic atlas of the tropical Indian Ocean", *NOAA Technical Memorandum*, ERL AOML-69.

Schott, F., Reppin, J., Fischer, J. and Quadfasel, D., 1994, "Currents and transports of the Monsoon Current south of Sri Lanka", *J. Geophys. Res.*, , **99**, C12, 25127-25141.

Shetye, S.R. and Shenoi, S.S.C., 1988, "The seasonal cycle of surface circulation in the coastal North Indian Ocean", *Proc. Ind. Acad. Science*, **97**, 53-62.

Simmons, R.C., Luther, M.E., O'Brien, J.J. and Legler, D.M., 1988, "Verification of a numerical ocean model of the Arabian Sea", *J. Geophys. Res.*, **93**, 15437-15461.

Yu, L., O'Brien, J.J. and Yang, J., 1991, "On the remote forcing of the circulation in the Bay of Bengal", *J.Geophys. Res.*, **96**, 20, 449-20, 454.